DEVELOPMENT OF TRANSPARENT WINDOWS FOR A NEW GENERATION OF CHERENKOV COUNTERS SENSITIVE IN THE EUV RANGE

A. Braem, G. Charpak, D. Drakoulakos, D. Fraissard,
Y. Giomataris, D. Hatzifotiadou*, G. Lecoeur and E. Rosso
CERN, Geneva, Switzerland

ABSTRACT

We present results concerning the development of windows transparent in the Extreme Ultraviolet (EUV) 10–50 eV range. These windows can be produced in large surfaces. Combined with gaseous photodetectors that have a solid photocathode or a photosensitive gas, they allow the exploration of an extended wavelength region. This allows efficient photon counting beyond the cut-off imposed by conventional far UV windows. Two different technologies are presented together with their performances in terms of far–extreme UV transmission, gas separation, and ageing properties. A simple monochromator capable of operating and performing measurements in the EUV range is also described. These windows can be used in various applications in particle physics and astrophysics, and especially for a new generation of simple and highly efficient Cherenkov counters and Hadron Blind Detectors.

1 Introduction

Threshold Cherenkov counters are widely used in high-energy physics for particle identification. Their spectral sensitivity, limited in the ultraviolet (UV) region by the transmission cut-off of the window material, often leads to a poor detectable Cherenkov light yield. Low-light yield is more serious for the highest momentum threshold. Thus a gas with a low refractive index (such as He) is required. However, this also imposes an increase of the radiator length. Cherenkov He radiators of about 10 m length have already been used in particle physics, especially those operating in the visible light region where the light absorption is negligible.

A way to decrease the length of the radiator is to increase the useful light yield by extending the spectral sensitivity to the far UV region by using expensive and delicate LiF windows. Another promising approach using windowless threshold Cherenkov counters has recently been proposed [1, 2]. The useful Cherenkov photon bandwidth is extended in the Extreme Ultraviolet (EUV) region up to the He ionization potential at 25 eV. In the new concept, the gas radiator is used simultaneously for electron multiplication in the well-known high-gain proportional operation mode of gaseous detectors. These detectors are called Hadron Blind Detectors (HBDs) because of their possible use in future hadron colliders, and their ability to select leptons by rejecting low-momentum hadrons. The HBD, being a threshold Cherenkov counter, can be used for particle identification in the Cherenkov threshold mode.

Extensive laboratory tests were needed to find gas mixtures that are transparent in the EUV region and that are compatible with the operation of gaseous detectors. Tests in 1990 showed that high-gain operation of Parallel Plate Avalanche Chambers (PPAC) having a CsI photocathode is possible by using He or Ne gas mixtures with CF_4 [3]. A prototype tested in a particle beam gave encouraging results and demonstrated the principle of this technique [4]. The main message from these results is the high Cherenkov quality factor obtained: $N_0 = 500$. This achievement opens a new frontier in Cherenkov technology and could lead to new improvements for building highly efficient threshold Cherenkov counters with moderate costs, low radiator length, a low number of channels, fast, and compatible with high-rate operation in future super-colliders.

A different approach is to try to separate the gas radiator from the photon detector. In order to achieve this it is necessary to develop thin windows that are transparent in the wavelength range of interest (40–120 nm) beyond the range covered by the most transparent monocrystals. Alternatively one could consider using a narrow microchannel plate which separates the radiator from the detector volume, producing a significant drop of pressure in order to limit the interdiffusion process from one volume to another at an acceptable low level. The latter two methods give a great flexibility for the new generation of Cherenkov counters, by giving the possibility to choose the desired gas for the radiator, and the ideal quencher for the photodetector. This gives the possibility of tuning directly the Cherenkov momentum threshold by selecting the gas-radiator filling and permits the use of highly efficient gases for the photodetector. The use of very transparent gases like He or Ne can enhance the number of detected Cherenkov photons, and very large quality factors can be obtained.

To get a feeling of the above, we have calculated the number of Cherenkov photons produced in a 20 cm long He or Ar radiator. The refractive index for each gas under normal temperature and pressure was calcu-

*Supported by World Laboratory, Lausanne, Switzerland.

lated from the data of Reference [5]. The energy range for the Cherenkov photons was 6–23.3 eV for He, and 6–13 eV for Ar. The upper limit in the photon energy range is given by the cut-off value in the Selmeir formula used for the calculation of the refractive index, and the cut-off at 6 eV is imposed by the CsI photocathode used as the photon converter. Figure 1 shows the number of photons produced by protons, kaons, pions, and muons as a function of the particle momentum. (1.a is for the He and 1.b is for the Ar radiator). The total number of Cherenkov photons emitted at saturation is 24 for the He, and 73 for the Ar radiator. Since a minimum of a few photons is required for efficient detection, even in the case of the lowest refractive index gas (He), the photon production is sufficiently high to take into account various losses caused by photoabsorption in the entrance window and the photocathode efficiency. We should also point out that in conventional Cherenkov He radiators the required length is of the order of 10 m. The range of identification covered by using the momentum threshold method widely takes into account the great flexibility of our procedure: the refractive index can vary in a wide range by mixing noble gases or by increasing (decreasing) the pressure.

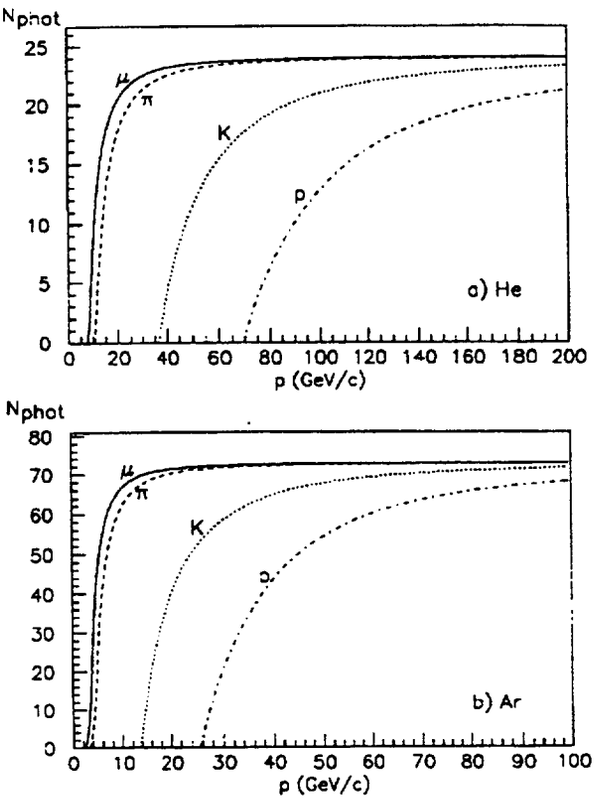

Figure 1: The number of Cherenkov photons produced by muons, pions, kaons, and protons as a function of the particle momentum for a) a He, and b) a Ar radiator, 20 cm long.

In the following sections we present details of these approaches. We describe the various experimental setups used for the measurements, results confirming the above ideas, and new developments and perspectives.

2 Microchannel plate gas separation

2.1 Description of the microchannel plate

The structure of the microchannel plate (MCP) consists of a glass plate with a thickness of 3 mm having cylindrical capillaries with a hole diameter of 26 μm, and a distance between two successive holes of 31 μm. The cylindrical holes have a slope of 7° with respect to the direction normal to the microchannel surface. This is relevant for the application of the MCP for electron multiplication in vacuum, in order to prevent the ion feedback. In our application the inclination is not useful and we are planning to suppress it in future prototypes. Taking into account the geometrical structure of the MCP, it was calculated that the open area is 64.2% in the optimal position (the position of the MCP for which the maximal cross section of holes occurs).

The effective transmission process of Cherenkov photons via the MCP depends on the relative angle between the direction normal to the MCP surface, and the direction of the emitted Cherenkov radiation, and consequently crucially affects the efficiency of the HBD. Thus, the accurate laying of the MCP in the HBD is necessary to obtain an optimal result. We have used two different techniques to measure the transmission and the angular acceptance of the MCP: the first using a laser, and the second using a monochromator, and these are described below.

The MCP was irradiated with a visible light beam of 630 nm wavelength, beam diameter 0.63 mm, and beam divergence 1.3 mrad, produced with an He–Ne laser; a photodiode was placed behind the MCP. The optimal position was localized, and afterwards the cut-off transmission angle was measured by rotating the MCP around the optimal position. Figure 2 shows the transmission of the MCP, in per cent for various angles around the optimal position. The maximum transmission of 56% is close to the calculated one, and the acceptance is 2°, which is sufficient to contain Cherenkov photons produced with smaller angles in most of the gaseous noble radiators. We are investigating the possibility of increasing the angular acceptance of the MCP by coating the holes with a suitable metal which has a high reflectivity at grazing angles.

A second set of measurements was made using a monochromator operating in the visible and the near

UV region. Figure 3 shows the light transmission of the MCP for various wavelengths and different angles in respect to the optimal position. The lower transmission, compared to the measurements with the laser, is caused by the significant beam divergence of the monochromator. As expected the transmission as a function of the wavelength is almost flat, so for the EUV region we should have a similar transparency.

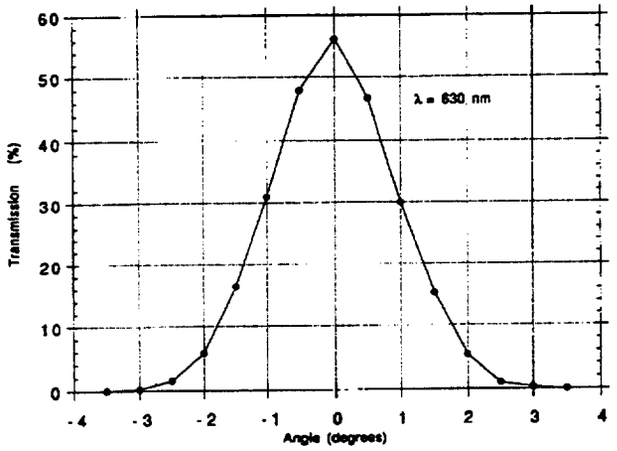

Figure 2: The transmission of the MCP for various angles of incidence of the light ($\lambda = 630$ nm from a He–Ne laser).

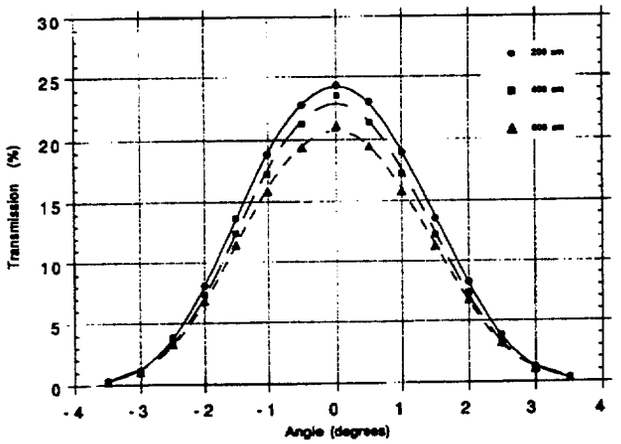

Figure 3: The transmission of the MCP for various angles of incidence of the light ($\lambda = 200$, 400, and 600 nm).

2.2 Gas separation

As mentioned in the first section, in order to optimize the operation of the Hadron Blind Detector it is necessary to separate the gas radiator from the detector volume. Laboratory tests were performed using a test prototype, shown schematically in Fig. 4. It consists of the radiator, 19 cm long with a 10×10 cm^2 transverse cross-section, supplied with a gas inlet E_2, and the MWPC, 1 cm long, supplied with a gas inlet E_1. Both sections have a common gas outlet S_1, and they are separated by the previously described MCP.

The experimental method of testing the gas separation was the following: we supplied different gases (argon, nitrogen, helium) with different volume flow rates at the radiator section, whilst keeping constant the volume flow rate of the MWPC section, which was supplied only with air. The oxygen contamination in the radiator volume was measured by an oxygen meter, having 0.2 ppm sensitivity, connected to a metallic probe S_2 (see Fig. 4). By suspending the probe with a springy system we were able to sample the oxygen concentration in different longitudinal (z-axis) and transverse (y-axis) positions.

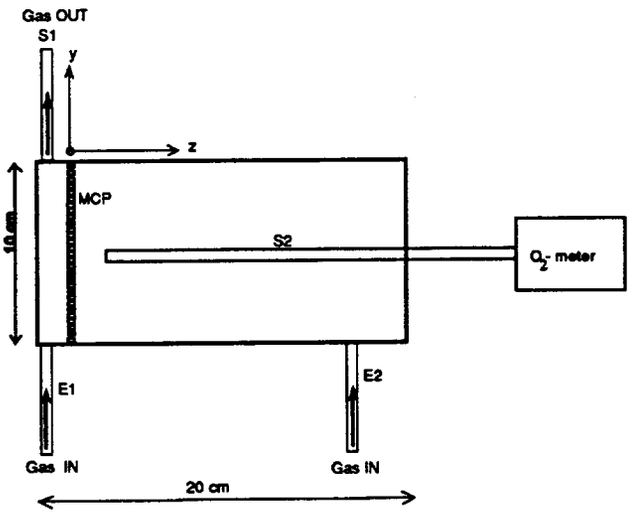

Figure 4: Schematic layout of the system used for gas separation measurements. Two compartments are defined by the MCP gas separator. The left compartment simulates the MWPC with gas input E_1 and gas output S_1. The right compartment simulates the radiator volume with gas input E_2. A metallic probe S_2 picks up a small fraction of the gas mixture and passes it to the oxygen meter.

Figure 5 shows the oxygen concentration for different flow rates (fixing the airflow rate at 4 l/h), for various gases at E_2. It can be concluded that the density of the radiator gas plays a dominant role in the diffusion process of oxygen in the radiator area via the multichannel plate.

From the data shown above, it can be concluded that the separation of gases between the two zones split up by a microchannel plate can be controlled by choosing suitable flow rates in both sections. Our goal is to keep the contamination at the level of 100 ppm, which seems feasible after the previous measurement. At that level,

absorption effects of various contaminants produce a negligible effect, and therefore in the case of Cherenkov radiation produced inside the vessel, photons can reach the detector volume with little attenuation. The photodetector will operate with a mixture of the tested noble gases, as the carrier gas, and a few per cent of an adequate quencher like methane, carbon monoxide, or other suitable gases. It could operate in the simple parallel plate mode, or in the multiwire proportional chamber mode. A first candidate as the photosensitive element is a layer of a solid CsI photocathode [16], which was proven to be compatible with gaseous detectors in high gain operation. A greater choice is, however, offered to us because of photon detection in the EUV region: in this range most of the quenchers used for gas amplification are at the same time very efficient photon converters, and thus a variety of gas mixtures is available. In this configuration we get rid of the ageing of the solid photocathode as well as the non-reproducibility of the quantum efficiency of CsI [7–16].

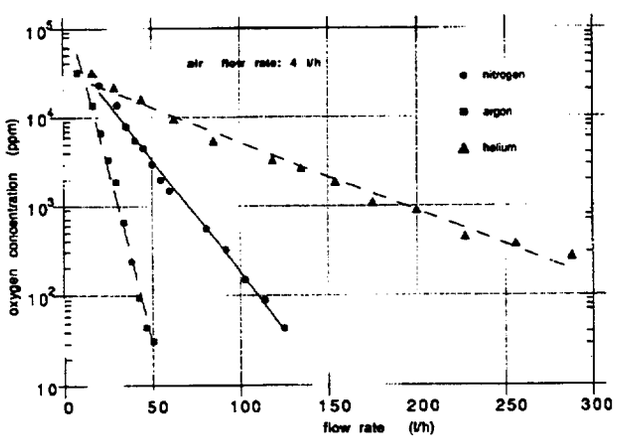

Figure 5: Oxygen concentration (in ppm) in the radiator section as a function of the flow rate at inlet E_2 using various gases (nitrogen, argon, and helium). The airflow rate at inlet E_1 was fixed at 4 l/h.

3 Thin window development

Even fluoride monocrystals are not transparente to the EUV light below 115 nm. In this region the typical light absorption lengths for common materials are of the order of a few nm, and require the use of thin membrane technology even for small surfaces. As an example, Fig. 6 shows the transmission as a function of the wavelength of a thin polyamide film, 42 nm thick, provided by Outokumpu Instruments Oy Company. Such a film was calculated to be fully transparent in the soft X-ray range [16]. In the visible region the maximum transmission is 38%, whilst in the far UV region it is only of the order of 5%. Taking into account the thickness of the film, the corresponding photon mean free path is roughly a few tens of nanometers in the visible region, and only a few nanometers in the far UV region, and therefore below the limit of the feasibility of such thin membranes.

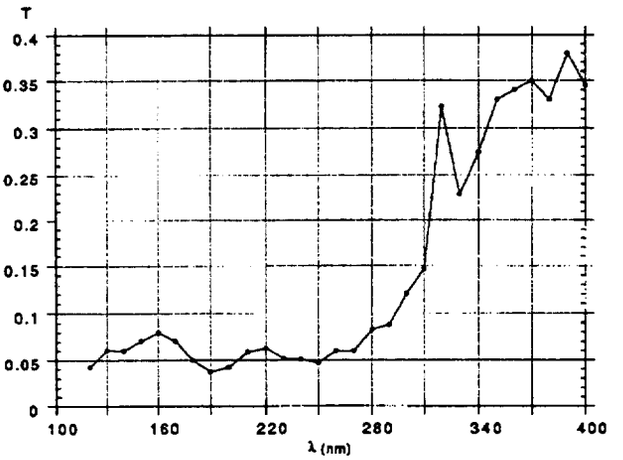

Figure 6: Transmittance of a 42 nm thick polyamide film.

Metals, however, show a very particular behaviour: they are good reflectors in the visible and the UV region due to collective effects of the free electron plasma; light penetrates a very short distance inside it and then is reflected. However, when the wavelength is in the domain of the plasma frequency, which is in the range of the EUV region for solid materials, then metals can suddenly transmit light, and their reflectivity drops. This leads to the terminology of ultraviolet transparency of metals. The light absorption length then becomes of the order of 1 μm, and thin film metal technology can be used.

We have developed such thin metallic windows which can be produced in large surfaces. The metallic film was supported by a nickel mesh having 20 μm holes and 75% transparency. A continuous film of 1 μm was first formed on the mesh by smearing it in a bath of a photoresistive polyamide. A first layer of magnesium 100 nm thick was deposited on the polyamide by vacuum deposition, followed by a second protective layer of indium 10 nm thick. After this the photoresistive polyamide was removed by dissolving it in an acetone bath. This development was made in collaboration with D. Berthet, A. Gandi and L. Mastrostefano of the CERN printed circuit workshop.

Because of the lack of windows transmitting in the EUV region, transparency measurements in this region need expensive and sophisticated monochromators working in the vacuum. We have modified a commercial cheap monochromator in order to operate at atmospheric pressure under noble gas circulation. The whole vessel

which contains the basic elements is flushed with gas. In the next section we give details of the various components.

3.1 The monochromator

The experimental arrangement used to measure transmisssion and the absorption of various materials is shown in Fig. 7. Light from a commercially available D_2 lamp having an MgF_2 crystal window is collimated by a 100 μm slit, and is reflected by a toroidal grazing grating with a grazing angle of $\theta = 32°$. The grating is made of a glass replica coated with metal, having 1200 grooves. We had two different gratings, one with aluminium coating with an MgF_2 protection layer, optimized for the wavelength range 100–300 nm, and a second one with platinum coating, having better sensitivity in the EUV region down to 50 nm. The light is focused by the grating on to a second slit, passes through a special cell where the thin windows are placed, and reaches the photodetector (PMT). We have adopted a readout of the PMT signal based on a photon-counting technique instead of a current measurement. We believe that this aproach gives an optimal signal-to-noise ratio since the minimum background level is the dark current counts of the PMT (200 Hz frequency). Taking into account that photon measurements are possible in the MHz repetition rate region, the dynamic range is wide by at least 4 orders of magnitude.

The basic monochromator used was model 302-VM of MINUTEMAN. The photodetector was an RCA-8850 quantacon photomultiplier with a pyrex window coated with a wavelength shifter and a bialkali photocathode. Two different coatings were used. The first was a p-terphenyl layer of 500 nm thickness, absorbing wavelengths in the 100–300 nm range, and emitting at 380 nm, where the PMT has the highest quantum efficiency [17, 18]. The second was sodium salicylate, a material which fluoresces in the sensitive area of the PMT when it is stimulated by vacuum ultraviolet radiation. A quite flat response of this shifter was observed in the far UV and the EUV [19]. Our test had little effect when p-terphenyl was replaced by the sodium salicylate and confirms older results.

Transmission measurements were performed by introducing the various samples into a specially designed chamber. It is located between the exit slit of the monochromator and the photodetector. The basic element of the test chamber is a cylindrical gas tight container, 3 cm thick, which has 8 locations carrying the samples for the transmission measurement. One of the test locations is empty and is used for measuring the intensity of the incident light I_0. By rotating the aluminium plate the transmitted light I can be measured in the 7 available locations. The transmission is defined as the ratio I/I_0 of transmitted to incident light, and is measured at different wavelengths. A standard connector allows independent gas filling and circulation through the test chamber. We must point out that in most of the measurements described we have used the same gas filling for the monochromator, the glow discharge lamp box, and the sample chamber.

Since our purpose is to explore the range between 50–200 nm, in the present set-up we were limited in the far UV region by the D_2 lamp window, made of MgF_2, which absorbs light below 115 nm. Figure 8 shows the spectrum of the D_2 lamp obtained by using the first aluminium grating. It exhibits a peak at 160 nm as expected, and it gives a useful spectrum down to 112 nm. In a modified version of our set-up we have succeeded in overpassing this obstacle. The D_2 lamp was replaced by a simpler discharge lamp having two tungsten electrodes. The whole monochromator was flashed with Argon, giving spectral lines down to 75 nm, or with He, emitting down to 50 nm. Figure 9 shows the spectrum of the discharge lamp in Ar atmosphere at normal pressure. Argon emission exhibits a clear peak in the 120–130 nm region and gives a useful spectrum down to 85 nm. For shorter wavelengths Argon gas was replaced by He gas.

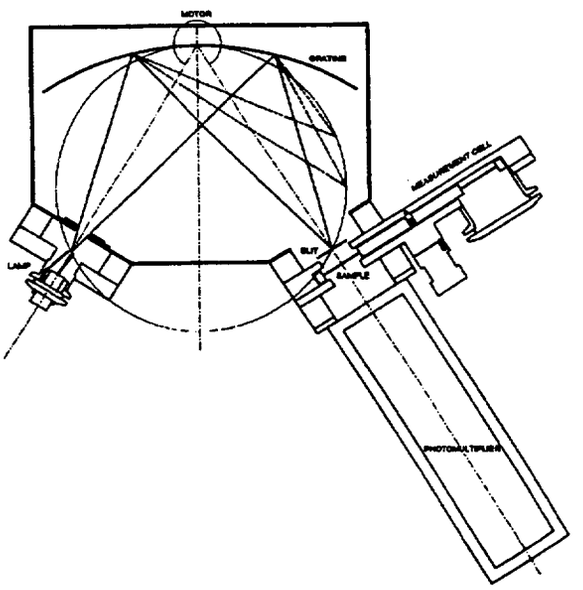

Figure 7: The principle of the monochromator. Light from a lamp is collimated by a slit, reflected by the monochromator grazing grating, focused by the grating on to a second slit, passes through a cell where the thin windows are placed, and reaches the photomultiplier.

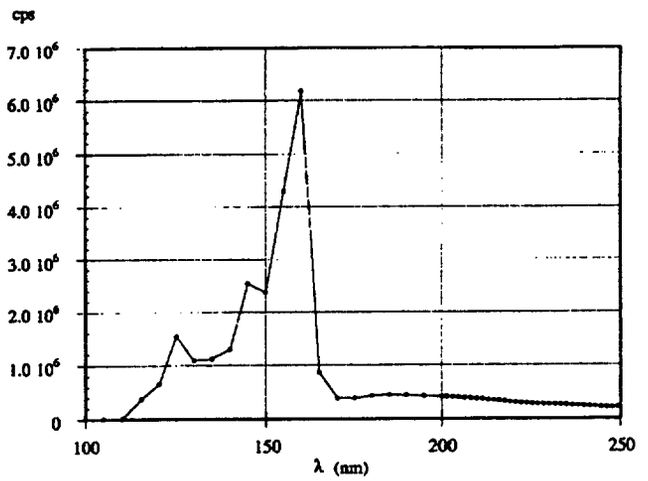

Figure 8: Spectrum of D_2 lamp with MgF_2 window.

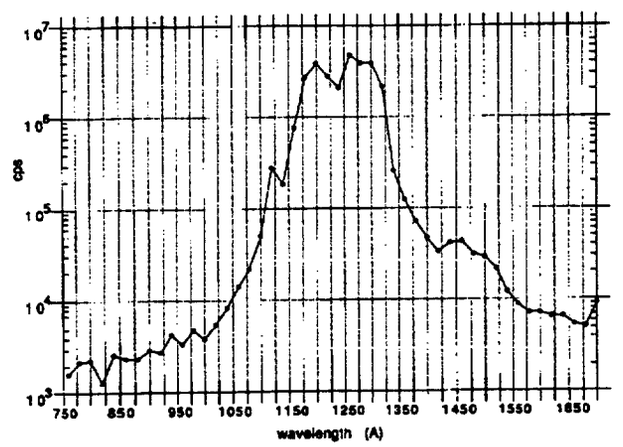

Figure 9: Spectrum of discharge lamp in Ar atmosphere.

3.2 Transparency measurements for metallic films

Measurements were made for the transmittance of light as a function of the wavelength for various thin metallic films. The first measurements were performed with Mg metallic films deposited by vacuum evaporation on a substrate of MgF_2, 1 mm thick. The transmittance is defined as the ratio between the number of photons that go through the sample and the number of photons through an MgF_2 crystal of the same thickness (1 mm) as the substrate. Figure 10 shows the transmittance of two samples, 50 nm and 100 nm thick. As expected from optical constant measurements [20] the Mg thin film is almost opaque in the visible and in the near UV region. In this wavelength region we observed a small amount of about 1% light transmission. This is due to inhomogeneities in the Mg deposition, some small light transmission through the thin metal, as well as some measurement uncertainties due to the low signal in this region. A significant transmission was observed below 190 nm for the 50 nm sample, and below 125 nm for the 100 nm sample. At shorter wavelengths the transmission increases and reaches 14% for the 50 nm film and 7.5% for the 100 nm film at the cut-off wavelength of 115 nm imposed by the MgF_2 substrate. This was the first encouraging result, demonstrating the capability of these metallic films to transmit light in the far and EUV region.

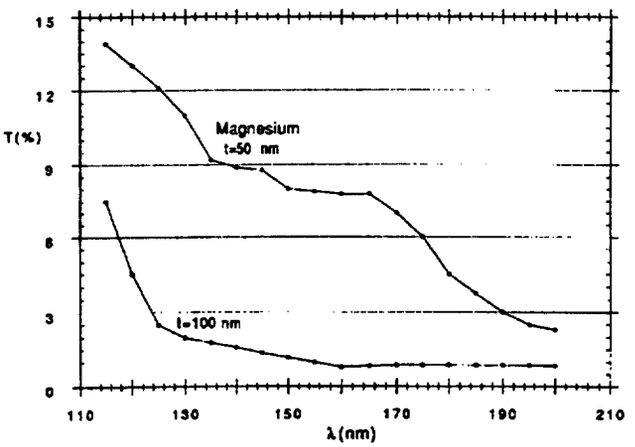

Figure 10: Transmittance of a 50 nm thick and a 100 nm thick Mg film deposited by vacuum evaporation on a 1 mm thick MgF_2 substrate.

We would now like to present some results concerning the ageing of the films. They are for two samples, both consisting of an Mg film of 52 nm thickness on an MgF_2 substrate of 1 mm thickness. In the second sample, in addition to the 52 nm of Mg there was an 11 nm MgF_2 layer, to act as protection against oxidation. Figure 11 shows the transmittance of the first sample, measured with the D_2 lamp, at various times up to 114 days after the deposition of the Mg layer. One can observe a degradation of transparency with time for the low wavelengths. This is due to corrosion phenomena: the deposition of a thin oxide layer on the metal surface results in a decrease of the light transmittance in the far UV region. Figure 12 shows the transmittance of the second protected sample at various times. One can observe that after four months of exposure to air and humidity the transmittance is practically unchanged. Therefore the 11 nm layer of MgF_2 is sufficient to protect against corrosion. This is an encouraging result, since the observed ageing effect was under hard conditions. In the real detector the metal will be in contact with clean gas since this is a requirement for optimal gas transparency. Therefore, the observed degradation of 20% of the protected sample should be taken as an upper limit.

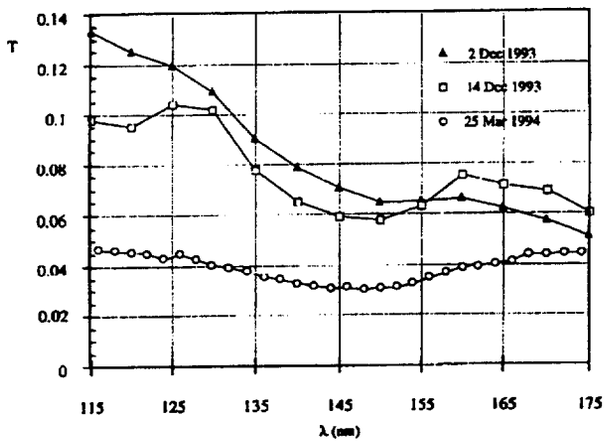

Figure 11: Transmittance of a 52 nm thick Mg film at various times (vacuum deposition on the MgF_2 substrate: 2 December 1993). Black triangles: 3 hours, white squares: 12 days, white circles: 114 days after deposition of the Mg film on the substrate.

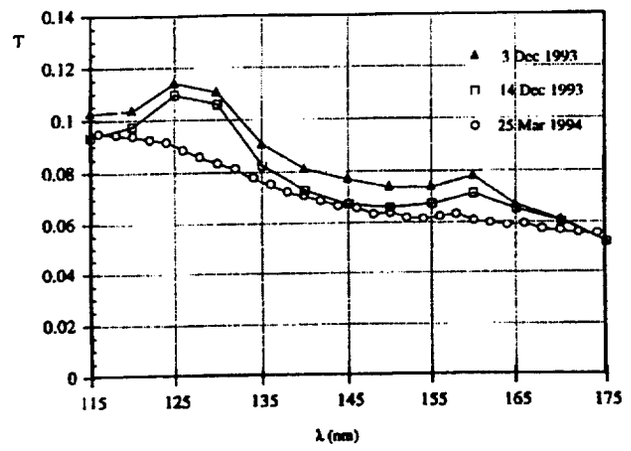

Figure 12: Transmittance of a 52 nm thick Mg film with an additional 11 nm protective layer of MgF_2 at various times (vacuum deposition on the MgF_2 substrate: 2 December 1993). Black triangles: 1 day, white squares: 12 days, white circles: 114 days after deposition of the Mg film on the substrate.

After the measurements for examining the ageing effects, we replaced the D_2 lamp with the glow discharge lamp giving a spectrum down to 85 nm in Ar gas, and 55 nm in He gas. Because of the cut-off at around 110 nm caused by the grating of the monochromator, we used a different grating (platinum) in order to cover the shorter wavelength region. In what follows we give results from measurements taken with this new grating.

The thin Mg 100 nm window protected with 10 nm. In made by the procedure described in Section 3, was introduced into the monochromator measurement cell after exposure in atmospheric air for 4 weeks. Figure 13 shows the transmission measured. In the visible and the near UV region the transmission is negligible: it starts to rise at about 120 nm and it reaches a value of 20% below 75 nm. The cut-off at 120 nm is certainly imposed by the In, whilst at shorter wavelengths the transparency is dominated by the Mg. We consider the result presented here to be a first satisfactory test. In the future it could be improved by more careful control of the properties of the different materials used, and a better adjustement of the various parameters during the coating processes. Moreover, we will try to reduce the minimum thickness of the film in order to increase further the light transmission.

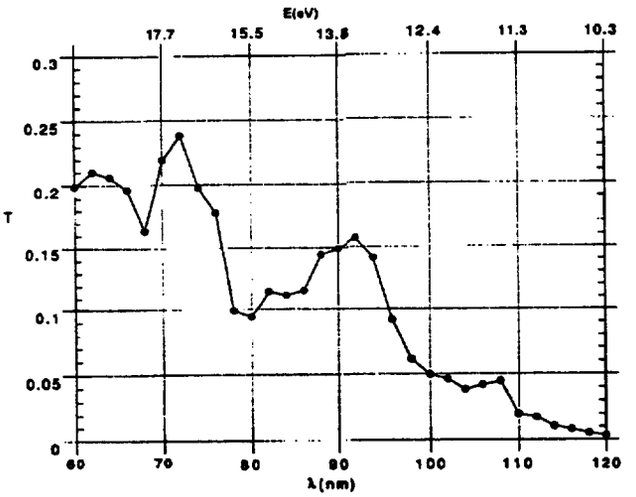

Figure 13: Transmittance of a 100 nm thick Mg window coated with 10 nm thick In layers on both sides. The wavelength shifter used for this measurement was sodium salicylate. Helium gas was circulated through the discharge lamp, the monochromator vessel, and the test cell.

4 Conclusions and outlook

A demanding program was undertaken towards the development of windows transmitting in the EUV region. Two different approaches were presented and experimental results exposed. Both techniques gave encouraging results and can be used for particle physics, space research, as well as in nuclear technology and medecine. They could be used with fully efficient gaseous photodetectors for single-photon counting in a difficult wavelength range between the UV and soft X-ray domain. We should now explore the full Cherenkov window offered by the most transparent noble gases, He and Ne. This will give an extraordinary gain in the Cherenkov technology allowing the construction of fast, inexpensive, minimum material, efficient counters, blind to direct ionization. A prototype based on this technology